



Research Article

A Method to Estimate Reflection Coefficient of Ultrasonic Wave at a Boundary of Two Media

Ryuugo Mochizuki¹, Yuya Nishida², Kazuo Ishii²

¹Center for Socio-Robotic Synthesis, Kyushu Institute of Technology, 2-4 Hibikino, Wakamatsuku, Kitakyushu, 808-0196, Fukuoka, Japan

²Department of Human Intelligence Systems, Kyushu Institute of Technology, 2-4 Hibikino, Wakamatsuku, Kitakyushu, 808-0196, Fukuoka, Japan

ARTICLE INFO

Article History

Received 27 November 2021

Accepted 01 February 2023

Keywords

Acoustic impedance

Ultrasonic

Hardness estimation

Internal reflection

Reflection coefficient

ABSTRACT

In food industry, shortage of workers is one of a serious problem. Automation of food handling is a critical nowadays. To alleviate the damage caused by food picking operation by robotic hand, we propose non-contact acoustic impedance estimation with ultrasonic wave, which should be preceded before the picking for optimization of grasp stiffness. We assume the correlation between hardness and acoustic impedance. That is, the harder the medium is, the larger the impedance should be. As cooked food, the unevenness of hardness should be considered. We made samples with media of different acoustic impedances, and experimented with ultrasonic to find the relation between reflection coefficient and hardness. As the result, reflection coefficient increased by 0.03-0.15 at the boundary of two media as the bottom medium is switched from urethane to Aluminum.

© 2022 The Author. Published by Sugisaka Masanori at ALife Robotics Corporation Ltd.

This is an open access article distributed under the CC BY-NC 4.0 license

(<http://creativecommons.org/licenses/by-nc/4.0/>).

1. Introduction

In Japan, employment opportunities for both sexes have steadily increased up to now. According to the report [1], housewife household has been decreased by nearly two million, while, dual-income households have increased by the same number. Single households have also increased (for elderly, about three million, for non-elderly, about 1.5 million) for 20 years recently [2]. As the market of Japanese prepared dishes, in 2018, the increase rate has grown up to 127.3[%] since 2009 [3]. From the point of view, the demand for prepared dishes can be assumed to have relation with the increase of single or dual-income households. If the increase of single or dual income households continues, the supply

of prepared dishes may run short, thus, automation of food process and packing are examples of crucial tasks.

Here, we propose to introduce non-contact hardness estimation with ultrasonic wave to optimize grasp stiffness, which precedes to the picking operation to realize safe food picking by a robot hand.

As cooked food, Unevenness of hardness should be considered. Here is an example of radish (Fig.1), which was cut into proper size (nearly 50[mm] x 50[mm] x 20[mm]) and heated with a micro wave oven for three minutes. We used rheometer to measure the strain and stress, then, found Young's Modulus of randomly selected locations on the radish. Young's Modulus varied depending on the locations as Table 1 shows. Furthermore, We estimated reflection coefficient by



Fig. 1 radish sample

Table 1 Unevenness of Hardness
(Young's Modulus)

Location Number	Young's Modulus [kPa]
1	1.8×10^4
2	2.8×10^4
3	1.4×10^4
4	2.1×10^4
5	8.3×10^4

overlapping two samples with different acoustic impedance, considering the value as hardness. Acoustic impedance is the product of density and sonic velocity. Larger reflection coefficient should be estimated at the location of neighboring media as the discrepancy of acoustic impedances is larger, which means harder medium reflects stronger acoustic wave.

2. Related Work

Machado et. al. have analyzed ultrasonic reflection to evaluate stiffness [4] of three different wood species by finding sonic velocity in indirect method (Here, transmitter and receiver are aligned parallel and attached on a surface of a timber) and compared the result of direct method (Transmitter and receiver are aligned face to face). The relative error rate was less than 10 % between the two method.

Cho et al. used five kinds of cheeses to determine mechanical properties (Young's modulus, hardness, Toughness) with ultrasonic wave. They improved stability of thickness and ultrasound velocity measurement As the result, depth of cheeses was estimated in 99.98[%] of accuracy, then high correlation (coefficient of determination $R^2 > 0.9, 0 \leq R^2 \leq 1$) was found between acoustic velocity and the mechanical properties of the cheeses [5],[6].

Satyam et al. estimated varying hardness of tomatoes over a time period from fresh to full ripen cycle of the crops [7].

However, to the best of our knowledge, no report of hardness estimation considering heterogeneity of hardness has been found. The heterogeneity usually orients from uneven heating of food during cooking process, thus, we should consider the case of soft interior with hard surface.

3. Proposed Method

3.1. Outline

Acoustic impedance $\zeta (\in \{\zeta_1, \zeta_2, \dots\})$ can be expressed by Eq. (1), with ζ and c , here, $\rho[\text{kg/m}^3]$ indicates density of sample [8].

$$\zeta = \rho c. \quad (1)$$

To analyze received wave, we consider arbitral samples as multiple joints of media as Fig. 2 shows (z_k denotes the surface of medium k). Acoustic impedance ζ_k of media k has the relationship with reflection coefficient r_k as indicated by Eq. (2)[9], which means larger reflection can be found as the difference of hardness is larger between sample k and $k-1$, under condition media k is harder than $k-1$.

$$r_{k-1,k} = \frac{\zeta_k - \zeta_{k-1}}{\zeta_k + \zeta_{k-1}}. \quad (2)$$

We treat all ultrasonic waves in voltage because sound pressure cannot be measured in [Pa] with receiver.

As the calibration (Environment is shown as Fig. 3), we estimate attenuation coefficient α_0 [Np/m] and voltage P_0 [V], which corresponds to sound pressure of emitted wave, and is the reference to find $r_{0,1}$ of samples, then obtain and treat emitted wave $p_{i,0}(t)$ in similar way as basis function for wavelet transform [10]. Received wave $p_r(t)$ can be regarded as summation of reflected waves $p_{r,k}(t)$ at different surfaces of media. $p_{r,k}(t)$ is expressed in two ways, that is modelled reflection $\hat{p}_{r,k}(t)$, and reflection $\psi_{r,k}(t)$ based on a waveform $\psi_{i,0}(t)$, which is the estimation of $p_{i,0}(t)$ and obtained from the direct wave under the environment (Fig. 3). The former expresses relationship between reflection coefficient r_k at the surface of medium k and attenuation coefficient α_k [Np/m] of amplitude inside medium k . ~~based on amplitude.~~ The latter can express waveform because $\psi_{i,0}(t)$ is stretched or compressed in two direction (time and amplitude) to fit $p_{r,k}(t)$ in this stage. The flowchart (Fig. 4) shows the procedure to analyze $p_r(t)$. First, the

amplitude of $p_r(t)$ is thresholded with fixed value T_P for the judgement. If the judgement is true, $\psi_{i,0}(t)$ slides in the time axis direction, then stretched or compressed in the ratio of A_k vertically and B_k horizontally so that the correlation between $\psi_{r,k}(t)$ and $p_r(t)$ is maximized.

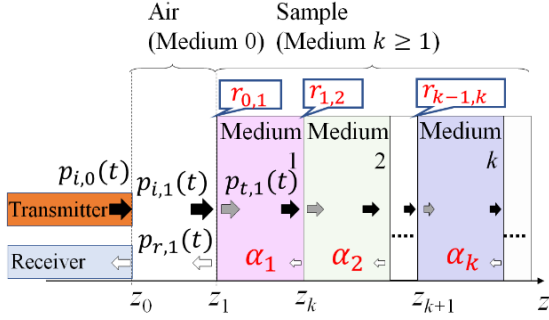


Fig. 2 Assumption of Sample Composition

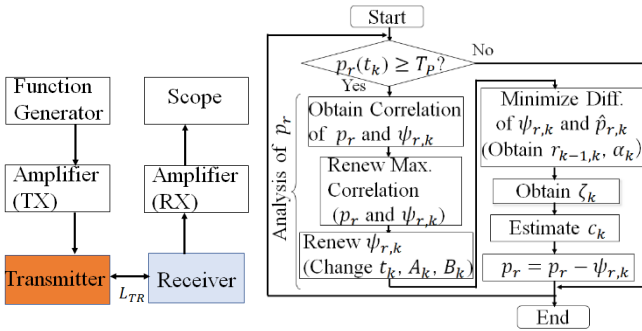


Fig. 3 Calibration Environment

Fig. 4 Process of Analyzing p_r

We limit searching area to find maximum of the correlation to $t_k > t_{k-1}$ (Here, t_k shows estimated time when $p_{r,k}(t)$ is received). At this stage, t_k should overlap the maximum amplitude of $\psi_{i,0}(t)$.

In the estimation of $\hat{p}_{r,k}(t)$, α_k and r_k are solved so that the squared error between $\hat{p}_{r,k}(t)$ and $\psi_{r,k}(t)$ is minimized. $\hat{p}_{r,k}(t)$ has another unknown parameter c_k [m/s] (sonic velocity in medium k), which is obtained through the fitting of linear function (the relation between sonic velocity c_k and acoustic impedance ζ_k , which is mentioned in Ref. 11). Hereafter, the estimation of α_k and $r_{k-1,k}$ continues as $p_r(t)$ is iteratively subtracted by $\psi_{r,k}(t)$ until amplitude of $p_r(t)$ drops below T_P .

3.2. Calibration of attenuation coefficient and sound pressure of the emission

Sound Pressure P_0 cannot be estimated in [Pa], then we assume that the pressure is proportional to output voltage [V] of the receiver. In calibration process, we find P_0 [V], α_0 [Np/m] to use in the analysis hereafter.

Function Generator generates one cycle of sign wave (Fig.5(a)) to the transmitter and direct wave is received as Fig.5(b) shows (Here, the direct wave is cropped to exclude reverberation.). P_0 and α_0 be calculated with the

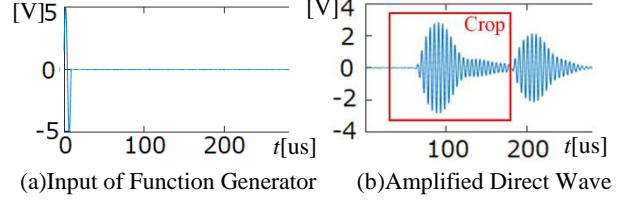


Fig. 5 Waveform of Direct Wave

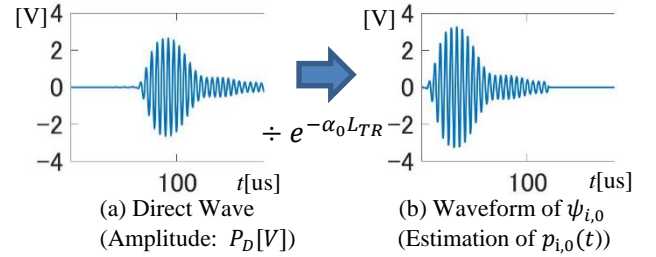


Fig. 6 Estimation of Emitted Wave $p_{t,0}$

amplitudes of directed waves that are observed from a few different distances L_{TR} [m] from the transmitter. When P_0 and α_0 are obtained, as Fig. 6 shows, cancellation of the attenuation by α_0 in direct wave Fig. 6(a) results in the solution of $p_{i,0}(t)$, that is, $\psi_{i,0}(t)$ (Fig. 6(b)).

3.3. Expression of the reflected wave

As we have mentioned in section 3.1, $p_{r,k}(t)$ is indicated in two ways, that is, $\hat{p}_{r,k}(t)$ and $\psi_{r,k}(t)$, which is made from the compression or stretch of $\psi_{i,0}(t)$.

As $\hat{p}_{r,k}(t)$, we consider the attenuation of ultrasonic wave originates from the reflection (The amplitude of the reflected wave narrows to the ratio $r_{k-1,k}$ at location $z = z_k$) and transmission (The transmitted wave travels in velocity c_k [m/s] and the amplitude narrows to the ratio of $e^{-\alpha_k(z_{k+1}-z_k)}$ at $z = z_{k+1}$ since its entry at $z = z_k$). After the emission of $p_{i,0}(t)$, the reflection and transmission are repeated $2k-1$, $2k$ times, each other. Thus, $\hat{p}_{r,k}(t)$ is expressed in Eq. (3), (4).

$$\widehat{p}_{r,k}(t) = r_{k-1,k} C_{\Pi,k} \psi_{i,0}(t) e^{-2\alpha_{k-1}(z_k - z_{k-1})}. \quad (3)$$

$$C_{\Pi,k} = \prod_{k'=1}^{k-1} (1 - r_{k'-1,k'}^2) e^{-2\alpha_{k'-1}(z_{k'} - z_{k'-1})}. \quad (4)$$

However, $\hat{p}_{r,k}(t)$ only expresses the relationship of two voltage levels between emission and reflection at t [sec]

under attenuation. Though the Function Generator outputs a cycle of sine wave, the direct wave is viewed as a group of waves with continuously varying amplitude, and frequency f_c [Hz] (same as central frequency of the transducer). For the reason, we form $\psi_{r,k}(t)$ by stretching $\psi_{i,0}(t)$ A_k times vertically and $1/B_k$ times horizontally so that the correlation between $\hat{p}_{r,k}(t)$ and $p_r(t)$ is maximized. Here, we consider the attenuation of amplitude and slight change of frequency after the reflection as Eq. (5) shows.

$$\hat{p}_{r,k}(t) = A_k \psi_{i,0}\left(\frac{t-t_0}{B_k}\right) \quad (5)$$

Maximum sound pressure is assumed to be measured at $t = t_0$ in case transmitter and receiver contact each other.

4. Experiment

As we mentioned in Chapter 1, hardness s is regarded as acoustic impedance, then ζ_k is considered to be uniform because the hardness is even in medium k , here, s is based on Asker Type C [12] and labelled on the package of purchases [13]. We regard a sample as a medium in the experiment. Now finding complicate hardness change with ultrasonic is difficult, thus, we simplify hardness heterogeneity with two different media of different hardness, jointed vertically.

The object of experiment is to configure the increase of $r_{1,2}$ as ζ_2 is far from ζ_1 regardless of different sample depth H_S (H_{S1}, H_{S2} for sample 1, 2 each other). Though $r_{k-1,k}$ is negative when ζ_k is lower than ζ_{k-1} , we only consider positive reflection coefficient. We moved the sample randomly so that the center of the sample is near the center between the receiver and transmitter. The displacement and ultrasonic emission/analysis were repeated alternatively for fifty times.

4.1. Calibration

To find $r_{0,1}$ from the acoustic model, P_0 and α_0 are required. We recorded amplitude of direct wave P_D using the environment shown in Fig. 3 and changing L_{TR} . We expect that P_D attenuates during the transmission between the L_{TR} [m] of interval as Eq. (6) shows. Under, $L_{TR} = L_{TR,1}$ in the equation, α_0 and P_0 are iteratively estimated for 20 times.

$$P_D(L_{TR}) = P_D(L_{TR,1})e^{-\alpha_0(L_{TR}-L_{TR,1})}. \quad (6)$$

As Eq. (6) shows, voltage level P_D of attenuates sharply as L_{TR} increases near the origin of the emission, thus, we selected L_{TR} as short distance as possible ($= 10..50$ [mm])The attenuation by α_0 is cancelled as Eq. (7) shows.

$$P_0 = P_D(L_{TR,1})e^{\alpha_0 L_{TR,1}}. \quad (7)$$

4.2. Environment

The environment for experiment and the samples for reflection estimation is shown in Fig. 7, Fig. 8(a), (b), (c), (d), (e), each other. Air was removed from the liquid to facilitate ultrasonic transmission. Dents and slight steep were seen in the sample surfaces. The truth of ζ and c is summarized in Table 2. Urethane Gel is made through

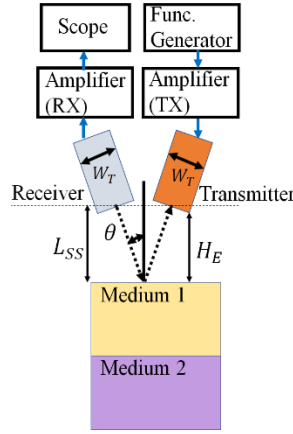


Fig. 7 Experimental Environment

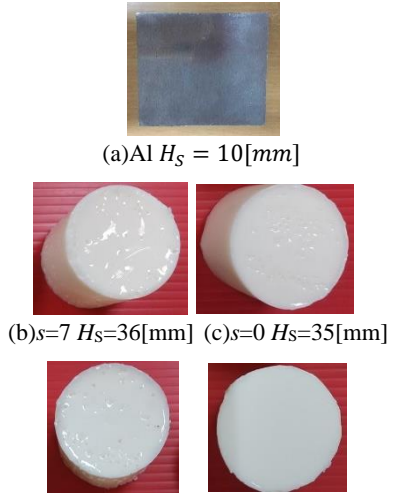


Fig. 8 Samples for the Environment

Table 2 True Value of Sonic Speed c and Acoustic Impedance ζ (at Temperature 30[deg])

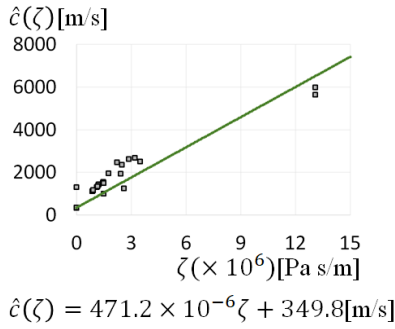
Sample Name	H_S [mm]	c [m/s]	ζ [Pa s/m]
Al	10	6420	17.3×10^6
Gel (s=0)	29	2237	2.5×10^6
	35	2233	2.4×10^6
Gel (s=7)	30	2185	2.5×10^6
	36	1643	1.8×10^6

Table 3 Setting for the Experiment

T_P	$P_0/100$	f_c	200[kHz]
H_E	50[mm]	τ	$\pm 40V$ (Calib.)21[deg]
θ_1	15[deg]		(Ref.)21[deg]
P_0	$\pm 40V$	3.07[V]	$\pm 50V$ (Calib.)21[deg]
	$\pm 50V$	3.27[V]	(Ref.)24[deg]
α_0	$\pm 40V$	2.43[Np/m]	a_1 471.1[m/(Pa s ² /m)]
	$\pm 50V$	1.52[Np/m]	a_2 349.8[m/s]

Table 4 Combination of Samples

Pattern	Sample 1		Sample 2	
	Sample Name	H_{S1} [mm]	Sample Name	H_{S2} [mm]
1	Gel ($s=0$)	29	Gel ($s=7$)	30
2	Gel ($s=0$)	29	Al	10
3	Gel ($s=0$)	35	Gel ($s=7$)	36
4	Gel ($s=0$)	35	Al	10

Fig. 9 Estimation of c with input of ζ

the mixture and coagulation of two different types of liquid. We solved true c by measuring elapsed time from wave emission to reception and dividing H_S with the time. As the true ζ , we substituted c in Eq. (1) to obtain. However, as ζ of aluminum, we referred to Ref. 11 because any metal has extremely large ζ . We repeated the calibration 20 times and averaged the voltage of the reception to find α_0 and P_0 . Table 3 shows the setting of this experiment (central frequency f_c , distance from transmitter and sample surface H_E , stilt of transducers θ_1 , temperature τ), and estimation of α_0 , P_0 . The amplitude of the input to transmitter was $\pm 40, \pm 50$ [V]. To find sonic velocity in media, we found simplified relationship of linear function between ζ and c , which is expressed with coefficients a_1, a_2 (Fig.9), a_1 differs from ρ in that a_1 is regarded uniform, while ρ synchronously changes as c changes. Table 4 shows the patterns of the sample combination, that is, material name, s, H_S .

4.3. Result and Discussion

The comparison of $r_{1,2}$ for pattern 1 and 2 is shown as Fig. 10, for pattern 3 and 4, as Fig. 11, which were recorded under condition that ± 40 [V] is input to transmitter. After that, we changed the amplitude of the

transmitter into ± 50 [V] to increase sound pressure. The result of $r_{1,2}$ are shown in Fig. 12 (pattern 1,2), and

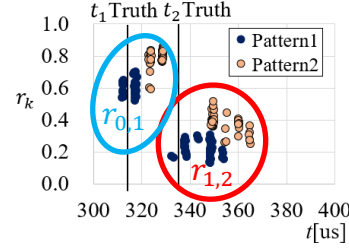
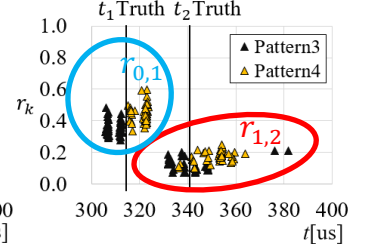
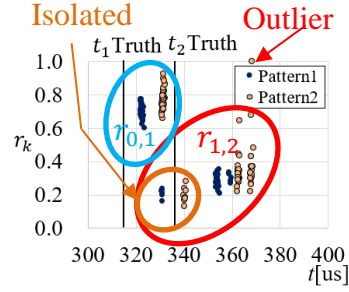
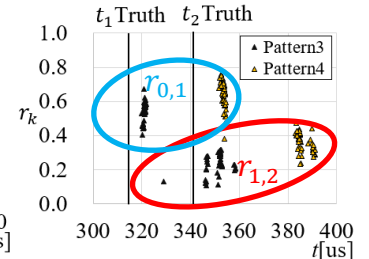
Fig. 10 Result of $r_{k-1,k}$ Estimation for Pattern 1, 2 (Input: ± 40 [V])Fig. 11 Result of $r_{k-1,k}$ Estimation for Pattern 3, 4 (Input: ± 40 [V])Fig. 12 Result of $r_{k-1,k}$ Estimation for Pattern 1, 2 (Input: ± 50 [V])Fig. 13 Result of $r_{k-1,k}$ Estimation for Pattern 3, 4 (Input: ± 50 [V])

Table 5 Summary of Reflection Coefficient Estimation Result

		Input ± 40 [V]	Input ± 50 [V]
Average of $r_{0,1}$ (50 times)	Pattern1	0.60	0.71
	Pattern2	0.79	0.76
	Pattern3	0.36	0.56
	Pattern4	0.45	0.64
Standard Deviation of $r_{0,1}$	Pattern1	0.05	0.04
	Pattern2	0.05	0.05
	Pattern3	0.05	0.06
	Pattern4	0.05	0.08
Average of $r_{1,2}$ (50 times)	Pattern1	0.22	0.29
	Pattern2	0.37	0.32
	Pattern3	0.15	0.24
	Pattern4	0.18	0.36
Standard Deviation of $r_{1,2}$	Pattern1	0.05	0.04
	Pattern2	0.06	0.10
	Pattern3	0.08	0.06
	Pattern4	0.03	0.05

Fig. 13 (pattern 3,4). True times of reflected wave reception are also shown in Fig. 10-13, which were

calculated with H_S and c . Table 5 shows the estimation result (average and standard deviation of $r_{0,1}, r_{1,2}$). The result of $r_{0,1}, r_{1,2}$ is surrounded by a blue, red oval in each figure (Fig. 10-13). As Table 5 shows, pattern 2 shows higher $r_{1,2}$ than pattern 1 and, pattern 4 shows higher $r_{1,2}$ than pattern 3, which means, increase of ζ_2 resulted in rising $r_{1,2}$. However, note that the average of $r_{1,2}$ is calculated without outlier in Fig. 12. Also, for Fig. 12, the distribution of $r_{1,2}$ was isolated (shown with an orange circle) apart. The 30[us] of delay in t_1 was shown in pattern4 of Fig. 13, which was mainly caused by heterogeneity of sample depth. To reduce the time difference between measured value and truth, bump or inclination of sample surface should be eliminated under coagulation.

5. Conclusion

We evaluated the effect of changing bottom media of samples into harder one (from urethane gel to aluminum).

As the result, we succeeded in finding larger $r_{1,2}$ according to the increase of ζ_2 , which may show the possibility of estimating the variety of hardness inside samples, however, the time of wave reception was not stable in the analysis.

References

1. "The Japan Institute for Labour Policy and Training," (in Japanese)
2. "Yahoo News" <https://news.yahoo.co.jp/byline/fuwaraizo/20130909-00027589> (in Japanese)
3. N. Kinoshita, "The Challenge for Sodium Reduction by Family Mart: Promotion of Unnoticed Sodium Reduction", (In Japanese), Japanese Society of Health Education and Promotion, Vol. 29, No. 3, 2021.
4. J Machado, P. Palma, S. Simoes, "Ultrasonic Indirect Method for Evaluating Clear Wood Strength and Stiffness", Non-Destructive Testing in Civil Engineering, pp. 1-6, 2009,
5. B. Cho and J. Irudayaraj, "Design and application of a non-contact ultrasound velocity measurement system with air instability compensation", Transactions of the American Society of Agricultural Engineers, Vol.46, No. 9, pp. 901-909, 2003.
6. B. Cho and J. Irudayaraj, "A Noncontact Ultrasound Approach for Mechanical Property Determination of Cheeses", Food Engineering and Properties, Vol.68, No. 7, pp. 2243-2247, 2003.
7. S. Srivastava, S. Vaddadi and S. Sadistap, "Non-Contact Ultrasonic Based Stiffness Evaluation System for Tomatoes during Shelf-Life Storage", Journal of Nutrition and Food Sciences, Vol. 4, Issue 3, pp 1-6, 2014.
8. J. Carlson, J. Deventer, A. Scolan and C. Carlander, "Frequency and Temperature Dependence of Acoustic Properties of Polymers Used in Pulse-Echo Systems", Proceedings in IEEE Symposium on Ultrasonics, pp. 885-888, 2003.
9. S. Takeuchi, Tutorial on the underwater or medical ultrasound transducer, (In Japanese) J. Acoust. Soc. of Japan, Vol. 72, No. 5, pp. 264-272, 2016.
10. R. K. Young, N. K. Bose, "Wavelet Theory and Its Applications", Kluwer Academic Publishers, 1993.
11. Honda Electronics Co., Ltd. "Ultrasound Handbook," (In Japanese), 2008.
12. "Kobunshi Keiki Co., Ltd. ASKER Durometer Type C".
13. "Exseal Co., Ltd. Hitohada no Gel Gen'eki" (in Japanese).

Authors Introduction

Dr. Ryuugo Mochizuki



He is a researcher at Graduate School of Life Science and System Engineering, Kyushu Institute of Technology, Japan. His research topic during the PhD course was image processing. Currently, he is involved in signal processing of ultrasonic.

Dr. Yuya Nishida



He is an Associate Professor at Graduate School of Life Science and System Engineering, Kyushu Institute of Technology, Japan. His research area is about filed robotics, its application, and data processing.

Prof. Kazuo Ishii



He is a Professor at Graduate School of Life Science and System Engineering, Kyushu Institute of Technology, Japan. His research area is about field robots and intelligent robot system
